



HAL
open science

pH-sensitive magnetic alginate/ γ -Fe₂O₃ nanoparticles for adsorption/desorption of a cationic dye from water

Delphine Talbot, Sebastien Abramson, Nébéwia Griffete, Agnes Bee

► To cite this version:

Delphine Talbot, Sebastien Abramson, Nébéwia Griffete, Agnes Bee. pH-sensitive magnetic alginate/ γ -Fe₂O₃ nanoparticles for adsorption/desorption of a cationic dye from water. *Journal of Water Process Engineering*, 2018, 25, pp.301-308. 10.1016/j.jwpe.2018.08.013 . hal-02016586

HAL Id: hal-02016586

<https://hal.sorbonne-universite.fr/hal-02016586>

Submitted on 12 Feb 2019

HAL is a multi-disciplinary open access archive for the deposit and dissemination of scientific research documents, whether they are published or not. The documents may come from teaching and research institutions in France or abroad, or from public or private research centers.

L'archive ouverte pluridisciplinaire **HAL**, est destinée au dépôt et à la diffusion de documents scientifiques de niveau recherche, publiés ou non, émanant des établissements d'enseignement et de recherche français ou étrangers, des laboratoires publics ou privés.

**pH-sensitive magnetic alginate/ γ -Fe₂O₃ nanoparticles for
adsorption/desorption of a cationic dye from water**

Delphine Talbot, Sébastien Abramson, Nebewia Griffete and Agnès Bée*

delphine.talbot@[sorbonne-universite.fr](mailto:delphine.talbot@sorbonne-universite.fr), nebewia.griffete@[sorbonne-universite.fr](mailto:nebewia.griffete@sorbonne-universite.fr),

sebastien.abramson@[sorbonne-universite.fr](mailto:sebastien.abramson@sorbonne-universite.fr), agnes.bee@[sorbonne-universite.fr](mailto:agnes.bee@sorbonne-universite.fr)

Sorbonne Université, CNRS, Laboratoire PHENIX, F-75005 Paris, France

* Corresponding Author :

Mail: agnes.bee@sorbonne-universite.fr

Tel: 33 1 44 27 30 98

Address: Sorbonne Université, laboratoire PHENIX, Campus Pierre et Marie Curie, case 51,
,4 place Jussieu, F-75005 Paris, France

Abstract

In this study, magnetic alginate nanoparticles (AlgMNP) were synthesized using a simple and green two-step method, which can be easily developed on an industrial scale. First, coprecipitation of both ferric and ferrous ions in alkaline medium followed by oxidation of magnetite into maghemite leads to a stable colloidal dispersion called ferrofluid. A sodium alginate solution was then added to the ferrofluid in order to obtain the magnetic nanocomposite. This approach combines the advantages of a biopolymer with magnetic properties of the maghemite nanoparticles. The morphology, structure, size and composition of the magnetic nanoparticles were characterized by means of atomic absorption spectrometry, transmission electron microscopy, X-ray diffraction, Fourier-transform-infrared spectroscopy and thermogravimetric analysis. Adsorption is one of the most efficient treatments for the removal of pollutants from wastewater. But the development of efficient and environmental friendly adsorbent still remains challenging. Using AlgMNP as a magnetic adsorbent could be a suitable response to this challenge. Its adsorption efficiency was investigated by using methylene blue as pollutant. The effects of pH, contact time, and initial concentration of the dye on adsorption were investigated. The high adsorption capacity with respect to the dye in a wide pH range (273 mg/g) was explained by the way magnetic nanoparticles bind to the alginate chains. We assumed an organization with alginate strands decorated by the magnetic nanoparticles leaving the adsorption sites of the particles more accessible rather than a configuration with a complete coating of magnetic nanoparticles by alginate. The reusability was successfully demonstrated through 10 adsorption/desorption cycles.

Keywords: Ferrofluid; alginate; maghsorbent; magnetic nanoparticles; adsorption; water remediation; dye

1 Introduction

Among the different technologies used for the removal of pollutants from industrial effluents, adsorption is considered to be an efficient and economic process easy to implement. However, the preparation of adsorbents that can efficiently remove pollutants, while exhibiting green properties and facilities for industrial development still remains challenging (1). Moreover, separating adsorbents from water after pollutants extraction remains a laborious and time-consuming step. Using magnetic adsorbents makes it possible to overcome these difficulties. Indeed, these materials can be easily extracted from the treated water by applying a simple magnetic process reducing the risk of secondary pollution of the environment by waste accumulation (2).

Magnetic nanoparticles and more particularly iron oxide nanoparticles have been widely studied and used since a long time in many fields such as hyperthermia, magnetic drug delivery, magnetic resonance imaging, data storage, environmental remediation and so on (3-8,9,10). These applications often need a surface engineering of the magnetic nanoparticles and the research of appropriate compounds to introduce additional functionalities to the nanoparticles attracts more and more attention. Nevertheless, it is still a challenge to synthesize functionalized magnetic nanoparticles in a controlled manner, especially when green and large-scale conditions are required (11).

Composites based on natural polymers are in focus as green adsorbents and among them, alginate seems to be a good candidate due to its strong adsorption properties. Alginate, mainly extracted from brown algae, is a water-soluble linear polysaccharide, which combines features of abundant resources, low-cost, biocompatibility and biodegradability. This natural polyelectrolyte is composed of β -D-mannuronate (M) and α -L-guluronate (G) units arranged in blocks rich in G units (G-block) or M units (M-block) separated by blocks of alternating G and M units (MG-block) (12). Alginates are extensively used in biotechnologies, medicine or food industry (13,14). It is mainly their gelling properties that are at the origin of their industrial applications. Due to this ability to form stable hydrogels, alginates can encapsulate different materials (15), which can strengthen their adsorption properties or confer them other properties, such as, for example, magnetic properties when magnetic nanoparticles are trapped in the polymer matrix (16-19). Therefore, alginate is currently a hot topic for environmental research and many polymer nanocomposites are developed for applications in this field (20-24).

Recently, different methods have been reported for the synthesis of magnetic alginate-nanoparticles (25-29). Two types of strategies are usually adopted: the magnetic nanoparticles

are either synthesized in-situ in the alginate matrix, or synthesized separately (co-precipitation, hydrothermal treatment, etc.) and subsequently added to the alginate solution (so-called two-step method). However, in most of these materials, magnetic nanoparticles consist in magnetite (Fe_3O_4), which is readily oxidizable and especially unstable in acidic environment (30), which complicates the regeneration of this kind of materials. In addition, they are mainly used for biomedical applications (28).

This study reports the synthesis of alginate/maghemite nanoparticles (AlgmNP) for the adsorption of water pollutants. The use of maghemite ($\gamma\text{-Fe}_2\text{O}_3$) instead of magnetite as magnetic core is of particular interest because of the much larger stability of this phase. In addition to the green character and the adsorption sites of alginate, magnetic properties of the nanoparticles allow their fast extraction from complex environmental samples with a simple magnetic process. The two-step method described here consists first in the preparation of size-controlled maghemite nanoparticles (MNP) dispersed in diluted nitric acid to form a stable ferrofluid. Alginate solution is then added to the ferrofluid to obtain the magnetic adsorbent. Alginate is bound to the surface of the MNP through its carboxylate functions; the remaining carboxylate groups can then be used to adsorb pollutants in water. This method, easy to implement, is an attractive approach for effective clean-up procedure because it does not use toxic products and can be developed at an industrial scale. Moreover, there is no need of centrifugation or filtration steps due to the magnetic properties of the materials used. The potential use of AlgmNP for water treatment was investigated through adsorption experiments, methylene blue being chosen as a model of pollutant. Dyes are compounds widely used in the industry and their presence in effluents is of serious concern because of their toxic effects for both environment and human health (31). The influence of pH, contact time, dye concentration on adsorption efficiency was studied. The reusability of the magnetic composite was demonstrated through adsorption/desorption cycles. We made a special effort to understand the interactions between the dye and the adsorbent. A good knowledge of our system and the control of the synthesis parameters enabled us to predict the number of active sites involved in the adsorption of the pollutant, which was then compared with the experimental results.

2 Experimental

2.1 Chemicals

Sodium alginate was purchased from Sigma Aldrich. The weight average molar weight (M_w) and the number average molar weight (M_n), obtained by gel permeation chromatography, are respectively 2.74×10^5 and 1.49×10^5 g/mol, leading to a polydispersity index (I_p) equal to 1.8.

The amount of carboxylate functions of alginate ($pK_a = 3.4-4.2$ (32,33)) was obtained from the dosage of their sodium counterions ($[Na]_{alg}$) by atomic absorption spectrometry with a Perkin–Elmer Analyst 100 apparatus. It is equal to 4.2 ± 0.1 mmol/g_{alg}.

Methylene blue (MB) was purchased from Sigma-Aldrich ($M=373.9$ g/mol). Stock solutions of MB were obtained by dissolving the powder in distilled water. Their concentrations were measured by spectrophotometry at $\lambda=664$ nm using a UV-Visible UVIKON XL Secoman apparatus; the extinction coefficient ϵ_{664} is 83243 molL⁻¹cm⁻¹.

2.2 Preparation of magnetic nanoparticles

A two-step procedure was used to obtain AlgMNP. In the first step, maghemite (γ -Fe₂O₃) nanoparticles (MNP) were synthesized according to the Massart's method (34,35) by alkaline co-precipitation performed by rapid addition of concentrated ammonium hydroxide (20%, 1L) in an aqueous stoichiometric mixture of FeCl₂ and FeCl₃ obtained by mixing 180 g of Fe(II) salt (0.9 mol) and 715 mL of Fe(III) solution (1.5 mol) in acidic medium (HCl). The resulting dark black magnetite (Fe₃O₄) was then stirred in nitric acid (360 mL, 2 mol/L), oxidized into maghemite by a boiling solution of Fe(NO₃)₃ (323g, 1.3 mol) and, after washing, dispersed into water leading to a stable magnetic fluid called ferrofluid. The pH value of the resulting suspension is about 2. At this time, nanoparticles are positively charged with nitrate counterions. In the second step, alginate solution (18 g/L) was added to the diluted ferrofluid to obtain the alginate-bound maghemite nanoparticles. Preliminary studies were carried out to optimize the ratio $R = \frac{m_{Alg}}{m_{MNP}}$ (m_{Alg} being the introduced weight of alginate and m_{MNP} , the weight of maghemite nanoparticles calculated from the iron concentration of the ferrofluid). Then, the reaction mixture was stirred for 30 min with an orbital shaker at 50°C. The alginate-bound maghemite nanoparticles were recovered from the reaction mixture by centrifugation (20min, 7500 rpm) or by using a permanent magnet with a surface magnetization of 800 G (typical value of the magnetic field at 1.5cm from a cylindrical Nd/Fe/B magnet with a diameter of 2.5cm and a height of 1cm). Then, nanoparticles were washed three times using distilled water and dried 48h in an oven at 70°C.

2.3 Characterization

The size and morphology of the magnetic nanoparticles were observed by transmission electron microscopy using a Jeol model JEM 100 CX at 100 kV. The magnetic size distribution of the nanoparticles, which can be approximated by a lognormal law, was obtained by fitting magnetization curves parameters and led to the mean diameter d_{Aim} (In

$d_{\text{Aim}} = \langle \text{Ind} \rangle$) and distribution width σ_{Aim} of the nanoparticles (36). The experimental device for the magnetic measurements was based on the one described by S. Foner (37). X-ray diffraction (XRD) on dried samples using a Rigaku Ultima IV apparatus with a copper anode (Cu K_{α} radiation, $\lambda = 1.54178\text{\AA}$) was performed to identify the crystallographic structure and size of the nanoparticles. The equivalent iron concentration of the ferrofluid ($[\text{Fe}]$) was determined by atomic absorption spectrometry using an air-acetylene flame (Perkin Elmer AAnalyst 100 apparatus). Before measurements, magnetic nanoparticles were heated to ebullition in concentrated hydrochloric acid ($\approx 12 \text{ mol L}^{-1}$) until total dissolution of the nanoparticles into iron (III) ions was achieved. The amount of alginate bound on nanoparticles was estimated from the thermogravimetric analysis (TGA) performed on dried nanoparticles in air atmosphere with a heating rate of $10^{\circ}\text{C}/\text{min}$ (TA Instruments SDT Q600). FT-IR spectra of pure alginate, MNP, and AlgMNP were recorded in KBr discs in the range of $4000\text{--}400 \text{ cm}^{-1}$ on a Bruker Tensor 27 to check the binding of alginate to maghemite nanoparticles.

2.4 Adsorption/desorption experiments

Batch adsorption experiments were carried out at room temperature ($\approx 20^{\circ}\text{C}$). 100 mg (m) of dried AlgMNP ($R=0.14$) were added to 10 mL (V) of MB at initial concentration C_0 , pH of the samples being adjusted using either HNO_3 or NaOH solutions. After stirring using an orbital shaker (IKA KS 260) (2h to reach equilibrium), nanoparticles were removed magnetically from MB solution. The concentration of MB remaining in solution at equilibrium (C_{eq}) or at a given time t (C_t) was measured by UV-Visible spectrophotometry at 664 nm. We checked for each measure that there was no change in the BM spectrum. In particular, no trace of alginate that could complex the BM appeared in the solution to be analyzed, which means that the AlgMNP retain their integrity during the various tests. The amount of adsorbed dye at equilibrium (Q_{eq}) or at a given time t (Q_t) was deduced using the mass balance equation $Q = \frac{(C_0 - C)V}{m}$.

For the desorption study, 100mg of AlgMNP were first added to 10mL of MB solution ($C_0 = 200 \text{ mg/L}$) at pH 7. After two hours of stirring, the nanoparticles were magnetically recovered, gently washed with distilled water and then introduced into 10 mL of nitric acid 0.01 mol/L for 30 minutes. The particles were again separated from the solution. The quantity of desorbed MB was then determined by UV-Visible spectrophotometry. Before the next

adsorption, the particles were washed to raise the pH to about 7. Ten adsorption/desorption cycles were carried out.

3 Results and discussion

3.1 Determination of the optimal concentration of polymer

At first, the optimal ratio $R = \frac{m_{Alg}}{m_{MNP}}$ needed to obtain an adsorbent with a high dye adsorption capacity was determined. For this, increasing amounts of alginate solution were added to a ferrofluid at an initial iron concentration $[Fe]_i=0.4 \text{ mol/L}$ ($m_{MNP}=640\text{mg}$), the total volume of the solution being 20 mL. Without alginate ($R=0$), the ferrofluid is a stable colloidal dispersion. Upon addition of alginate, a progressive flocculation of the ferrofluid occurs (Figure 1), which was followed by the determination of the iron concentration in the supernatant ($[Fe]_s$) (Figure 2).

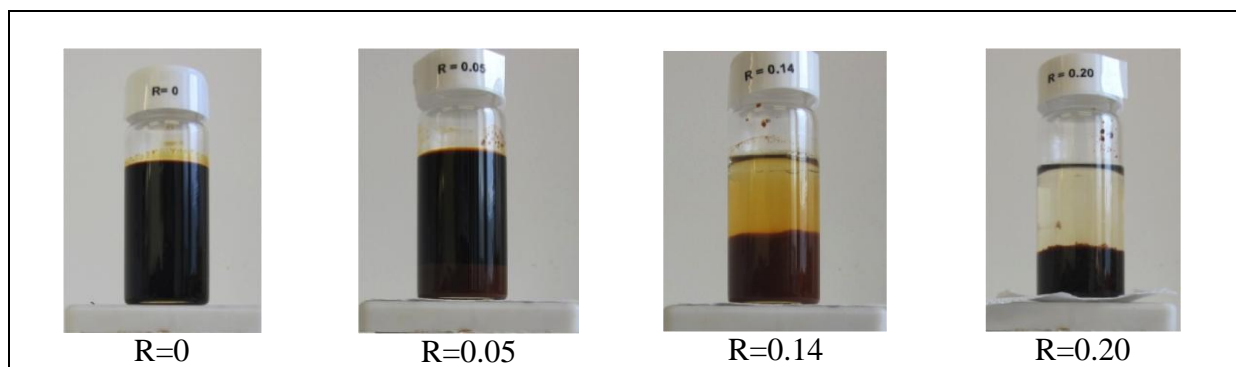


Figure 1: Effect on the amount of alginate on the stability of the ferrofluid.

For $R > 0.14$, flocculation is complete, there is no more nanoparticles in the supernatant, which appears colorless. This macroscopic phase separation was also followed by measuring the height of the brown precipitate (h). These measurements were carried out at equilibrium after leaving the samples on a magnet. As can be seen in Figure 2, h remains roughly constant for $R > 0.14$.

--	--

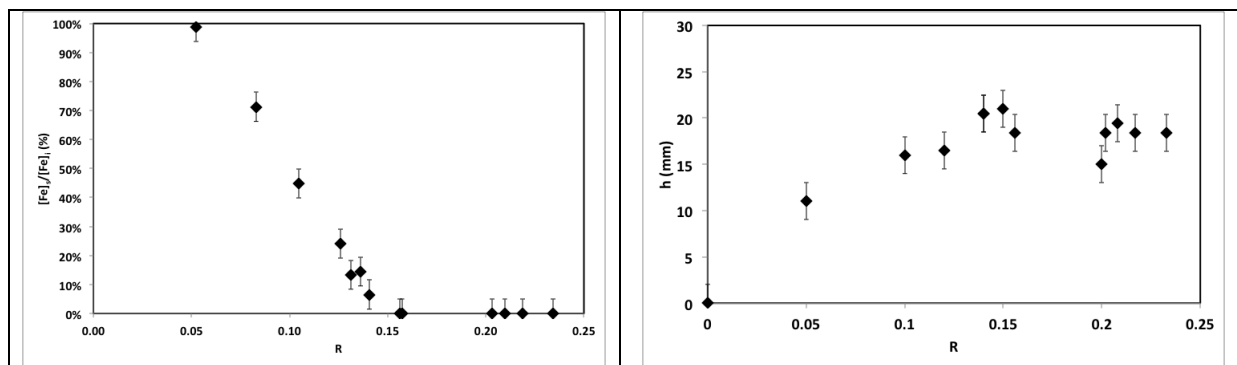


Figure 2 : Evolution of iron remaining in the supernatant ($[Fe]_s/[Fe]_i$) and of the height of the precipitate (h) with R (inner diameter of the bottle = 2.7 cm).

The stability of the ionic ferrofluid used is due to electrostatic repulsions between the charged nanoparticles. Without alginate, the charges of the nanoparticles come from the ionization of hydroxyl groups at their surface. The surface charge is positive for a pH value below the point of zero charge (PZC) of the nanoparticles and negative for pH above the PZC. The ferrofluid flocculates for a pH value close to the PZC; for maghemite, the PZC is located around pH 7 (38). The pH of the ferrofluid used in the samples being close to 2, nanoparticles are positively charged with nitrate counterions. By adding alginate, a self-assembly between negatively charged alginate and positively charged nanoparticles occurs involving the carboxylate functions of alginate; the surface charge of the nanoparticles decreases and the ferrofluid flocculates. In conclusion, we retained $R=0.14$ for the preparation of magnetic alginate nanoparticles.

3.2 Characterization of the magnetic nanoparticles

Magnetic nanoparticles were carefully characterized before investigating their adsorption properties. The iron concentration of the ferrofluid determined by atomic absorption spectrometry is 1.7 mol L^{-1} . A typical transmission electronic microscopy (TEM) picture of this diluted ferrofluid before alginate addition shows that the shape of the magnetic nanoparticles is roughly spherical. The analysis of the TEM pictures with the free software ImageJ leads to a mean diameter d_{TEM} equal to 7.6 nm with a polydispersity of 0.5.

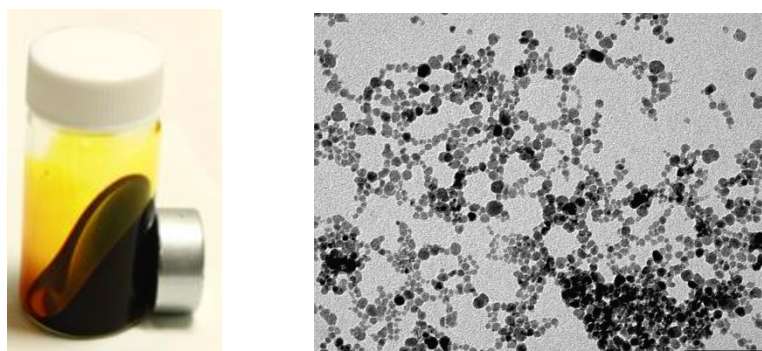


Figure 3 : A stable ferrofluid (left) and MNP picture obtained by transmission electron microscopy (right)

The mean diameter (d_{Aim}) and the polydispersity index (σ_{Aim}) of the naked nanoparticles were also obtained from a two-parameter fit of the magnetization curve of diluted ferrofluid (39); they are 7.4 nm and 0.4 respectively.

X-ray diffraction patterns (XRD) of MNP and AlgMNP are displayed in Figure 4. The characteristic peaks related to the crystal planes (220), (311), (400), (422), (511) and (440) are consistent with the data in JCPDS 39-1346 file corresponding to the maghemite structure. It is worth noting that the AlgMNP exhibit the same characteristic peaks as the naked MNP, indicating that alginate did not alter the crystalline phase of iron oxide. The average diameter of the nanoparticles, d_{RX} , calculated through full width at half maximum of the strongest reflexion of the diffractograms, using the Scherrer equation, is 7.7 nm for both MNP and AlgMNP.

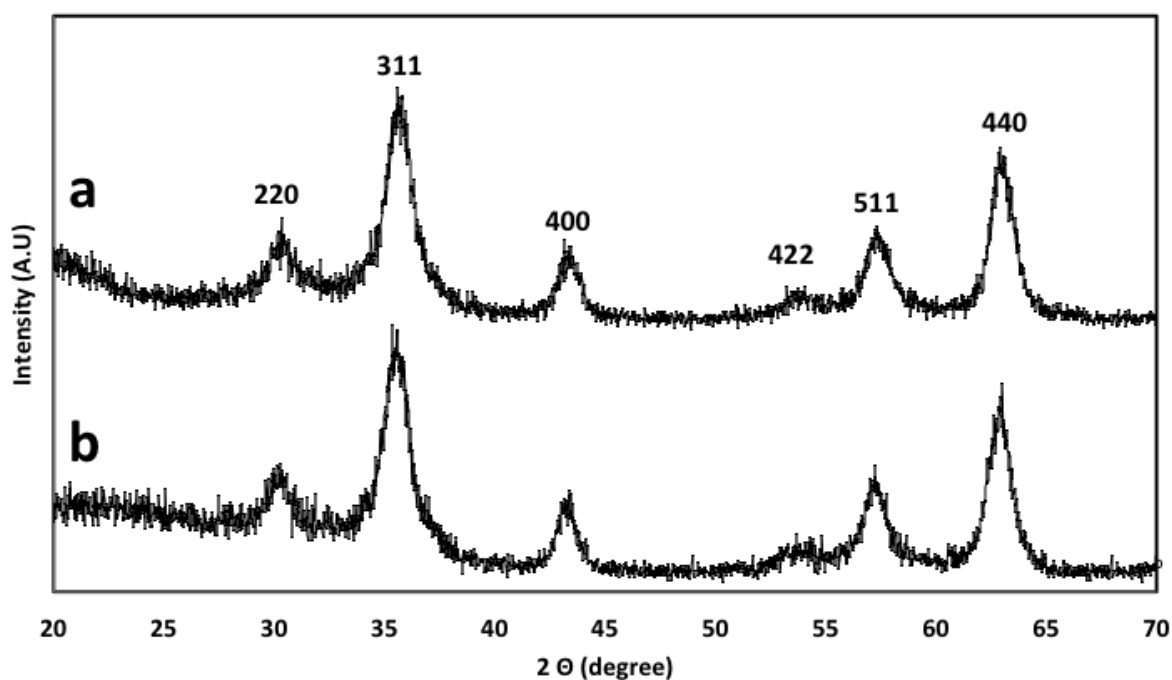


Figure 4 : XRD of AlgMNP (a) and MNP (b)

Evidence of the binding of alginate to the nanoparticles was provided by FT-IR analysis. The spectra of pure alginate, MNP and AlgMNP are shown in Figure 5. The corresponding characteristic bands and their attribution are listed in Table 1. The broad bands in the range $2600-3600\text{ cm}^{-1}$, present in the three spectra, can be attributed to stretching vibrations of -OH bonds of alginate and sorbed water on nanoparticles. The weak peak at 2920 cm^{-1} on the alginate spectrum is assigned to $-\text{CH}_2$ groups. Alginate also displays characteristic bands at 1618 and 1420 cm^{-1} corresponding to the asymmetric and symmetric stretching vibrations of

the carboxylate, respectively. The bands at 1094 and 1026 cm^{-1} are attributed to C-O bond in -C-OH groups. The bands at 581 and 631 cm^{-1} observed on the MNP spectrum are the signature of the Fe-O bonds. Moreover the intense narrow band at 1385 cm^{-1} is related to the nitrate counterions of the MNP. The small band at 1621 cm^{-1} is probably due to the deformation vibration of adsorbed water. The AlgMNP spectrum exhibits the characteristic bands from both alginate and MNP. The alginate carboxyl absorption bands are slightly shifted to 1609 and 1408 cm^{-1} probably due to the modification of the carboxyl environment, sodium ions being replaced by surface iron from MNP. However, no significant shifts are observed for Fe-O bands. The most notable change is the strong decrease of the nitrate band due to the replacement of nitrate ions by carboxylate from alginate. These results indicate that alginate was successfully bound to the MNP.

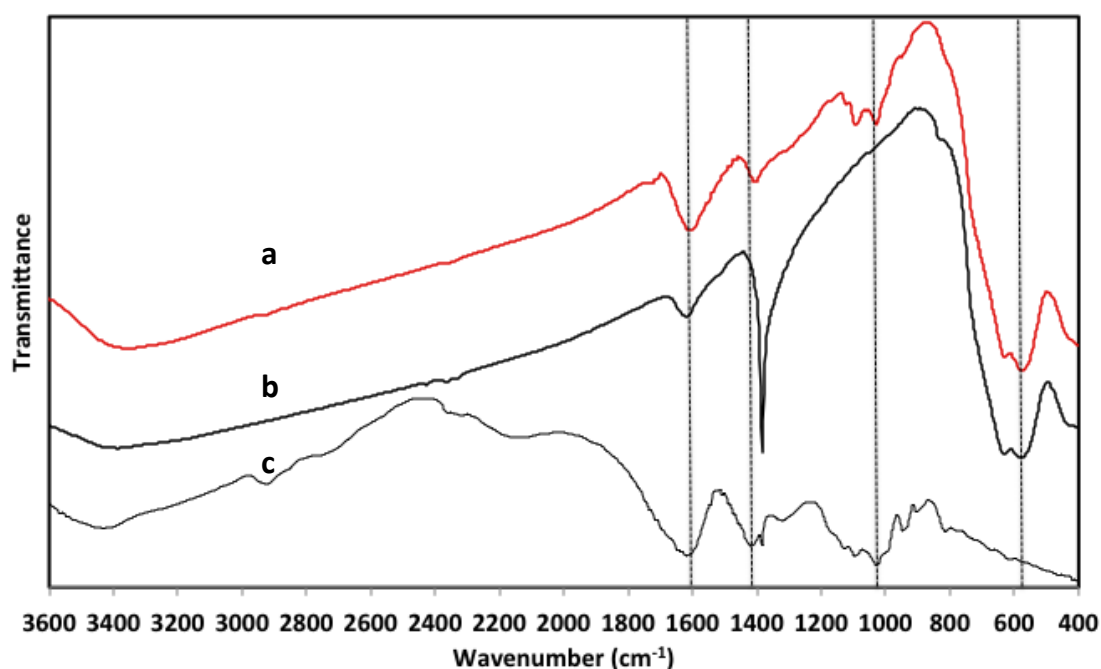


Figure 5 : FT-IR spectra of alginate (a), MNP (b) and AlgMNP (c).

Wavenumber cm^{-1}	Assignment
Alginate	
3431	O-H stretching vibration
2920	Aliphatic C-H stretching vibration
1618 and 1420	Asymmetric and symmetric stretching vibrations of carboxylate groups
1094 and 1026	Stretching vibration mode of C-O bond in C-OH groups
MNP	
3385	Stretching vibration of hydroxyl groups of sorbed water
1621	Deformation vibrations of adsorbed water

1385	NO ₃ ⁻ antisymmetric stretching mode
581 and 631	Stretching vibration of Fe-O bond
AlgMNP R=0.14	
3360	O-H stretching vibration (alginate and sorbed water on MNP)
1609 and 1408	Asymmetric and symmetric stretching vibrations of carboxylate groups of alginate
1094 and 1030	Stretching vibration mode of C-O bond in C-OH groups of alginate
576 and 629	Stretching vibration of Fe-O bond (MNP)

Table 1: FT-IR analysis of alginate, MNP and AlgMNP (25,26,29,40-42).

In order to calculate the amount of alginate bound to the MNP, we used thermogravimetric analysis (TGA). Figure 6 displays the curves from 20°C to 500°C for alginate, MNP and AlgMNP. TGA curve of MNP exhibits weight losses of 6% (up to 150°C) and 4% (between 150°C and 360°C) due to physically and chemically adsorbed water respectively. The alginate curve shows a first weight loss of 18%, between 50°C and 200°C, which corresponds to the water desorption and to the destruction of glycosidic bonds. Beyond 250°C, the glycosidic bonds were further destroyed (43). The total weight loss for alginate is 60%. In the case of AlgMNP, a weight loss of about 7% was observed from 20°C to 180°C due to the loss of water. In the second stage (180-360°C), the weight loss is about 9%, which was assigned to the thermal degradation of alginate adsorbed onto the surface of the maghemite nanoparticles. These results show that AlgMNP are stable below 180°C and that the samples contain 84±1 wt.% of γ -Fe₂O₃ and 9±1 wt.% of alginate. Thus the weight ratio of bound alginate to maghemite nanoparticles is 0.11. This value is slightly higher than reported values obtained for the coating of magnetite nanoparticles by alginate (29,40). From the density of the maghemite ($\rho=5.074$ g/cm³) and the average molecular weight of alginate ($M_w=200,000$ g/mol), it was estimated that 0.4 alginate chains on average were bound to each nanoparticle or about 2.6 nanoparticles were bound to each alginate chain. A similar result was obtained with PAA-magnetite nanoparticles ($M_{w,PAA}=180,000$ g/mol); the authors have shown that about 2 PAA were bound to one particle (44). In our case, it is probably more accurate to consider alginate chains decorated with nanoparticles rather than an alginate coating around the nanoparticles. AFM images obtained by Ma et al. showing magnetite nanoparticles bound to the strands of alginate macromolecules corroborate this assumption (26).

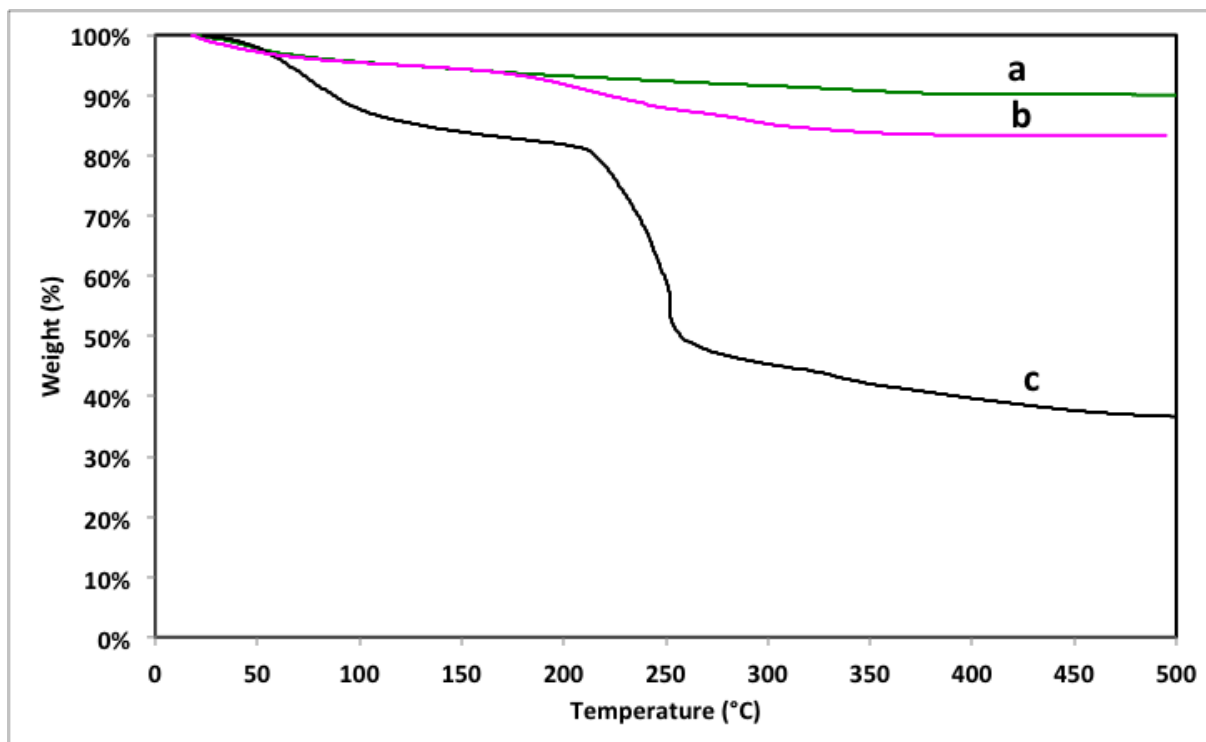


Figure 6 : TGA curves of MNP (a), AlgMNP R=0.14 (b) and pure alginate (c).

3.3 Adsorption studies

a. Effect of pH on MB adsorption

The charge and adsorption properties of the adsorbent are strongly affected by the pH of the solution. Hence, batch equilibrium studies were performed over a pH range from 2 to 11.2 to investigate the effect of pH on the adsorption of MB ($C_0=200\text{mg/L}$) by AlgMNP (Figure 7).

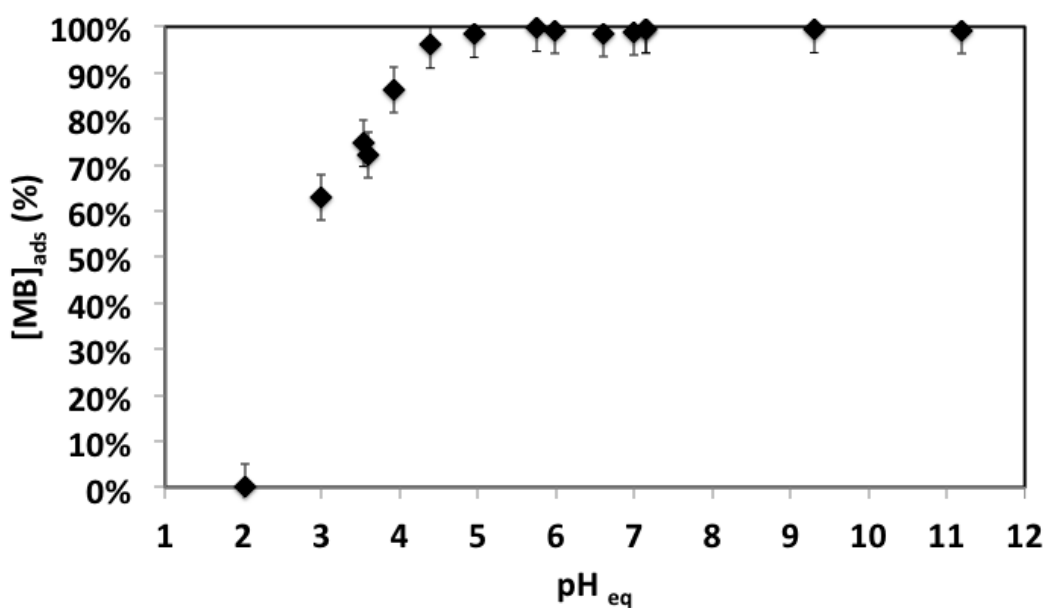


Figure 7: pH effect on MB adsorption ($C_0=200\text{mg/L}$)

The amount of adsorbed MB increases from 0 to 98% adsorption with increasing pH from 2 to 5, and this can be attributed to the ionization of carboxylate groups of alginate, which interact with the positively charged dye via strong electrostatic interactions. In addition, electrostatic repulsions between carboxylate groups expand the alginate chains making the adsorption sites more accessible to the dye (42). For $\text{pH} < 4.5$, the carboxylate protonation becomes significant and the adsorption falls, no adsorption occurs at $\text{pH} \leq 2$ while 100% adsorption is obtained in a large pH range [4.5-11.2]. The shape of the curve is characteristic of the adsorption of positively charged species by adsorbents carrying carboxylate groups (44,45). Due to the strong adsorption, the following studies were conducted at a fixed pH greater than 5.

b. Adsorption isotherm

The adsorption capacity of AlgMNP was determined by equilibrium adsorption experiments conducted at two pH values (7.1 and 10.1) (Figure 8).

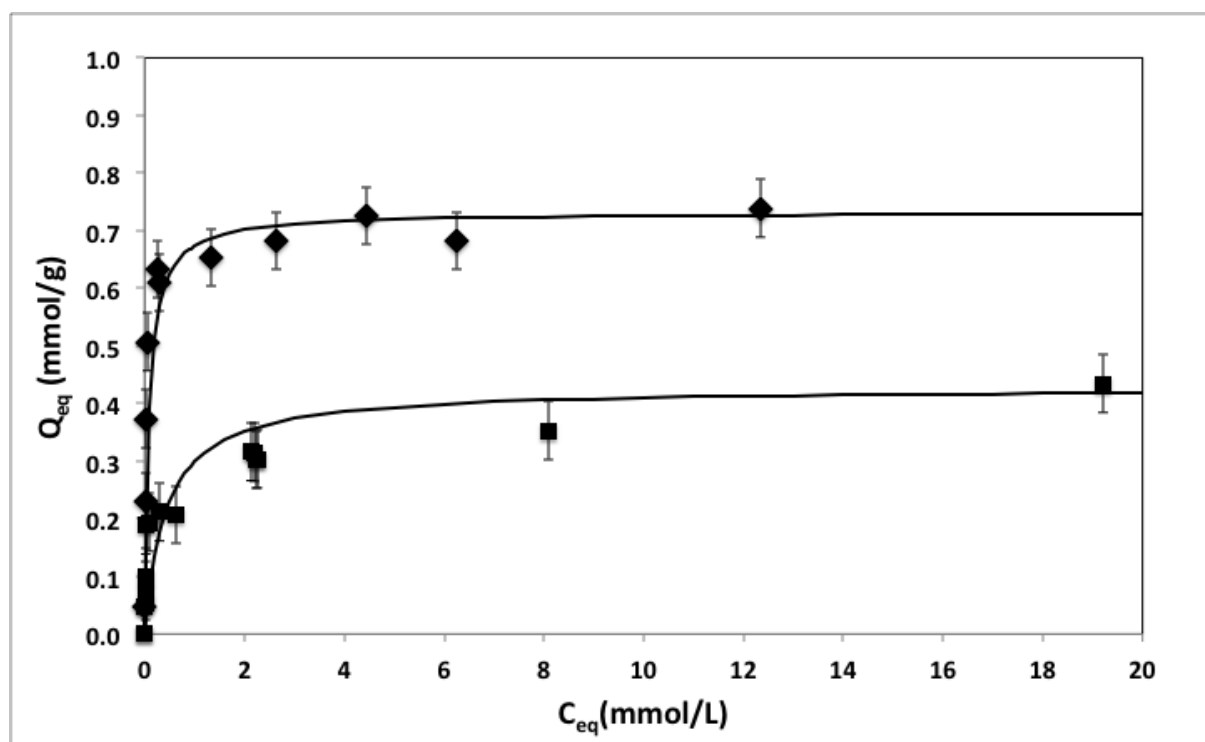


Figure 8 : Adsorption isotherms of MB onto AlgMNP, solid line represents the Langmuir isotherm; $\text{pH} = 10.1 \pm 0.5$ (\blacklozenge), $\text{pH} = 7.1 \pm 0.3$ (\blacksquare)

In both cases, the amount of adsorbed MB increases with increasing concentration of dye until reaching a plateau, which corresponds to the maximum adsorption capacity of AlgMNP.

A Langmuir equation was used to fit the experimental data. Its linearized form is $\frac{C_{eq}}{Q_{eq}} = \frac{1}{Q_{max}K_L} + \frac{C_{eq}}{Q_{max}}$, where Q_{eq} , is the amount of adsorbed dye at equilibrium, Q_{max} , the maximum adsorption capacity, C_{eq} , the concentration of dye in the solution at equilibrium and, K_L the Langmuir constant. Figure 8 and Table 2 prove that adsorption of MB on AlgMNP is well described by the Langmuir model. The maximum adsorption capacities obtained from Langmuir equation, 0.73 mmol/g at pH 10.1 and 0.43 mmol/g at pH 7.1 are very close to the experimental values.

pH	R ²	Q _{max}		K _L L/mmol
		mmol/g	mg/g	
10.1± 0.5	0.999	0.73	273	11.6
7.1± 0.3	0.989	0.43	161	2.3

Table 2 : Langmuir parameters

The adsorption sites of AlgMNP originate from both the carboxylate functions of the alginate bound to the particles and the nanoparticles themselves, which bear positive charges in acid medium and negative charges in basic medium. The amount of carboxylate functions of alginate was estimated to be 0.57 mmol/g from the mass ratio of bound alginate to maghemite taking into account that each monomer of the alginate carries one carboxylate function. A part of these carboxylate functions is used to form bonds between the alginate chains and the nanoparticles while the remaining part is available to adsorb the dye. On the other hand, the amount of adsorption sites of alginate-free MNP for a given pH value had been estimated previously by potentiometric measurements (46). At pH 7.1, close to their point of zero charge, the naked nanoparticles are not charged. Therefore, at this pH value the adsorption sites of AlgMNP originate only from the carboxylate functions of the alginate bound to the nanoparticles (0.57±0.05mmol/g). However, the maximum adsorption capacity (0.43 mmol/g) is lower than the amount of carboxylate functions because a part of them is used to form bonds with the nanoparticles. At pH 10.1, the magnetic nanoparticles, negatively charged, may also adsorb BM. This is why the maximum adsorption capacity is greater at pH 10 than at pH 7. At pH 10, the amount of negative adsorption sites of the MNP is 0.27 mmol/g (38). As for alginate, some of these sites are involved in binding with alginate, the remaining part being available for adsorption of BM. At this pH, the estimated maximum number of adsorption sites of AlgMNP is therefore 0.84±0.05 mmol/g, which is close to the maximum adsorption capacity of AlgMNP deduced from the isotherm (0.73 mmol/g). The difference could be explained by the mobilization of a part of the sites for the adsorption of alginate on

the nanoparticles. It could be noted that AlgMNP sites are about three times greater than for the magnetic nanoparticles without alginate.

The presence of available sites on the MNP agrees with our previous assumption of a polymer decorated with magnetic nanoparticles rather than a coating of alginate around the nanoparticles, which would mask their adsorption sites. Compared to other results from the literature, the maximum adsorption capacity of AlgMNP obtained in this work is either of the same order of magnitude or higher (17, 27, 47-48).

c. Effect of contact time

The kinetics of MB adsorption by AlgMNP was investigated. Figure 9 illustrates the effect of contact time on the adsorption of MB with two initial concentrations C_0 equal to 2008 and 1479 mg/L at an initial pH close to 7. Adsorption is very rapid since 80% adsorption occurs in the first 15 minutes. Thereafter, adsorption becomes slower to reach an equilibrium time equal to 2h. The adsorbed amounts at equilibrium are in agreement with the adsorption isotherm at pH 7. The rapid adsorption is due to the availability of the active sites on the adsorbent at the initial stages. Moreover, as already mentioned above, at pH 7 the deprotonated carboxylate functions repel each other and allow easier access for the dye molecules. The gradual occupancy of the sites decreases the efficient interactions between MB and carboxylate and the adsorption becomes slower.

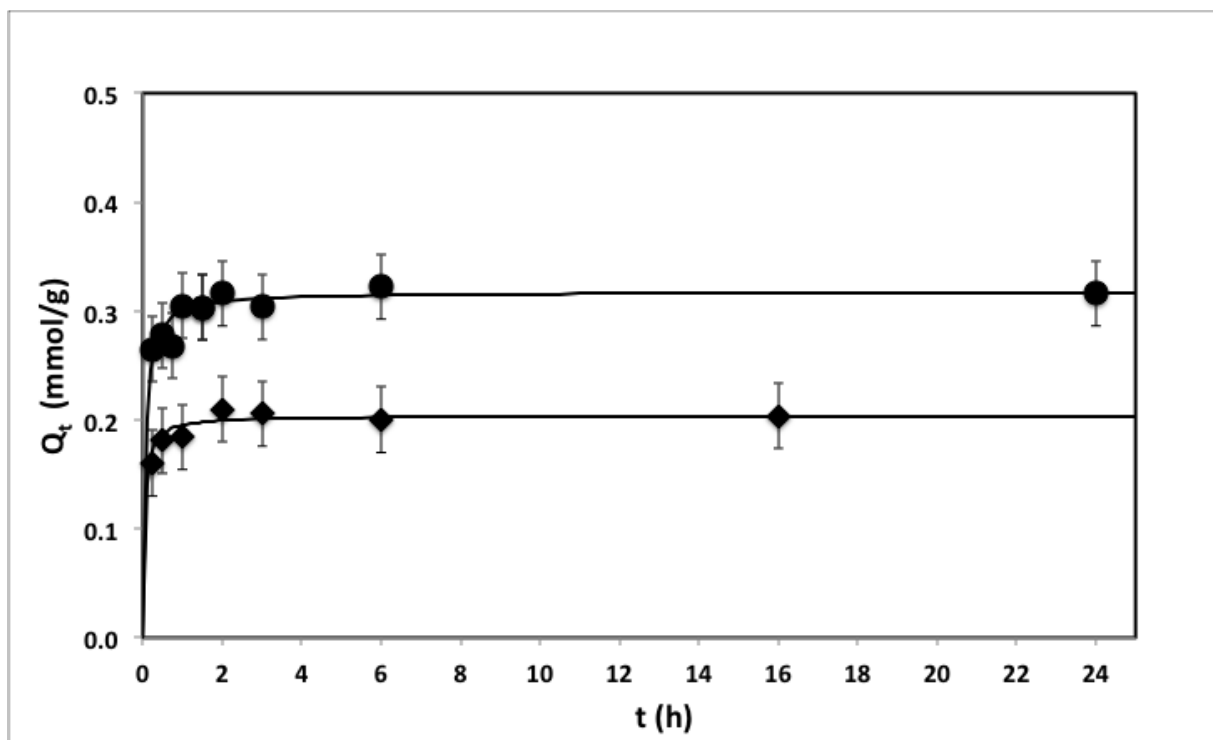


Figure 9 : Influence of contact time on MB adsorption: $pH=6.7\pm 0.3$, $C_0=2008\text{mg/L}$ (●); $pH=7.2\pm 0.4$, $C_0=1479\text{mg/L}$ (◆).

3.4 Reusability of AlgMNP

Reusability of AlgMNP is one of the key factors in evaluating the performance of an adsorbent. In order to investigate the reusability of AlgMNP, an adsorption/desorption cycle was repeated 10 times using the same nanoparticles. Carboxylate being protonated in acid medium, no more interactions occur between alginate and the dye and adsorption falls. Therefore, nitric acid at pH 2 was used as desorption agent. As it can be seen on the Figure 10, the amount of desorbed MB is greater than 99% and the adsorption capacity remains close to 100% even after 10 cycles. This result shows that the magnetic alginate nanoparticles could be used in a water treatment process without significant loss of their adsorption efficiency.

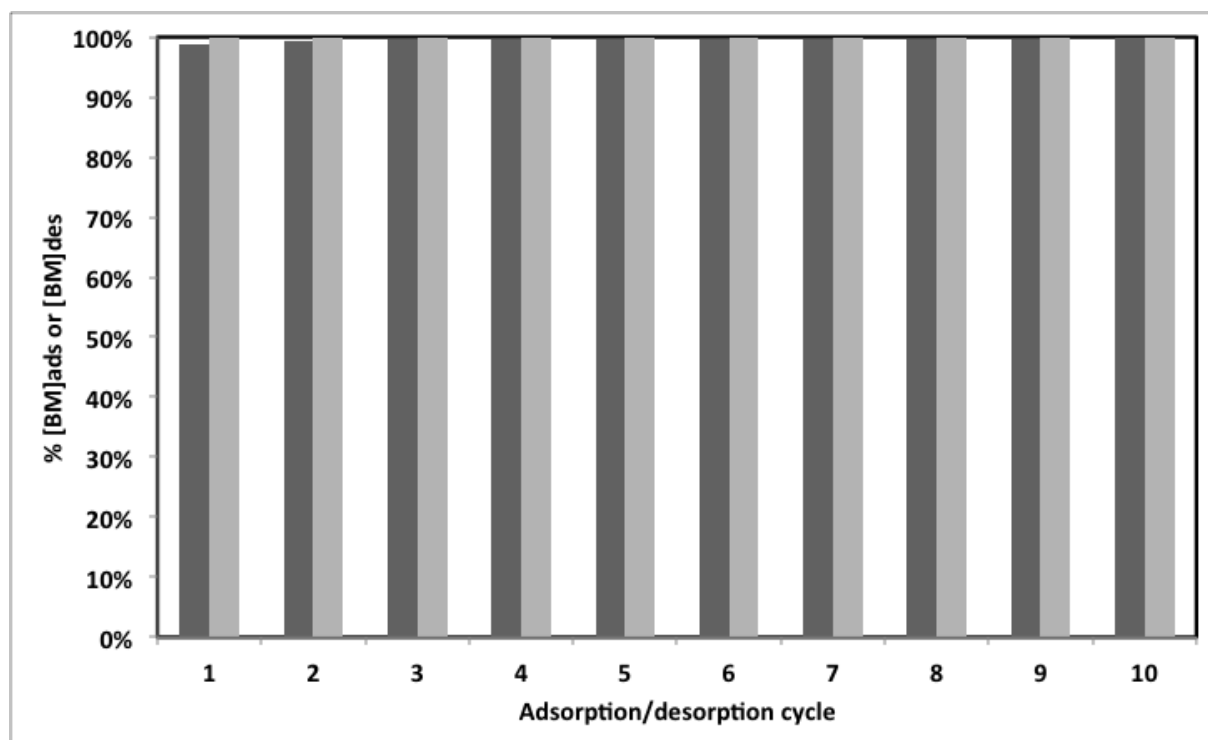


Figure 10: successive sorption (black) /desorption (grey) cycles

4 Conclusion

In this work, a magnetic adsorbent (magsorbent) based on an alginate nanocomposite with controlled particle size was prepared using a two-step method, which may be easily developed on an industrial scale. The combination of maghemite nanoparticles and a natural polymer such as alginate is one of the most promising methods to obtain a green adsorbent for the removal of pollutants from wastewater. This approach presents several advantages: maghemite has excellent stability with respect to oxidation; in addition, its magnetic properties makes it easy to recover after wastewater treatment by using a simple magnetic process; on the other hand, alginate is not only an abundant natural resource but its many

carboxylate functions ensure both a efficient binding to the nanoparticles and a strong adsorption capacity for cationic pollutants. Synthesized nanocomposites were carefully characterized before being used for the removal of a cationic dye (methylene blue) from water. The adsorption efficiency was increased at higher pH values because of the strong electrostatic interactions between carboxylate functions of alginate and cationic dye. The highest adsorption is at a neutral or basic pH. The maximum adsorption capacity of MB by AlgMNP is 273mg/g. The contribution of both MNP and alginate to the adsorption of the dye has therefore been envisaged and an organization with magnetic nanoparticles bound to the alginate chains through their carboxylate functions rather than a coating of MNP by alginate was proposed. The reuse performance of AlgMNP was higher than 98% even after 10 adsorption/desorption cycles. We can conclude that this study could be helpful in the development of magnetic adsorbents. AlgMNP present a high application potential for the recovery of cationic pollutants from water due to its magnetic properties, its adsorption efficiency and its reusability.

Acknowledgements:

The authors are very grateful to Mohamed Hanafi for GPC determination of molecular weights of alginate.

References

1. Ali I, Asim M, Khan TA. Low cost adsorbents for the removal of organic pollutants from wastewater. *J Environ Manage.* 2012 Dec 30;113:170–83.
2. Mehta D, Mazumdar S, Singh SK. Magnetic adsorbents for the treatment of water/wastewater—A review. *J Water Process Eng.* 2015 Sep;7:244–65.
3. Bayramoğlu G, Arica MY. Kinetics of mercury ions removal from synthetic aqueous solutions using by novel magnetic p(GMA-MMA-EGDMA) beads. *J Hazard Mater.* 2007 Jun 1;144(1–2):449–57.
4. Chen H-W, Chiou C-S, Chang S-H. Comparison of methylparaben, ethylparaben and propylparaben adsorption onto magnetic nanoparticles with phenyl group. *Powder Technol.* 2017 Apr 15;311:426–31.
5. Su C. Environmental implications and applications of engineered nanoscale magnetite and its hybrid nanocomposites: A review of recent literature. *SIEnvironmental Nanotechnol.* 2017 Jan 15;322, Part A:48–84.

6. Caetano BL, Guibert C, Fini R, Fresnais J, Pulcinelli SH, Menager C, et al. Magnetic hyperthermia-induced drug release from ureasil-PEO-[gamma]-Fe₂O₃ nanocomposites. *RSC Adv.* 2016;6(68):63291–5.
7. Neveu S, Bee A, Robineau M, Talbot D. Size-Selective Chemical Synthesis of Tartrate Stabilized Cobalt Ferrite Ionic Magnetic Fluid. *J Colloid Interface Sci.* 2002 Nov 15;255(2):293–8.
8. Ngomsik A-F, Bee A, Talbot D, Cote G. Magnetic solid–liquid extraction of Eu(III), La(III), Ni(II) and Co(II) with maghemite nanoparticles. *Sep Purif Technol.* 2012 Feb 15;86:1–8.
9. Demarchi CA, Debrassi A, de Campos Buzzi F, Nedelko N, Ślawska-Waniewska A, Dłużewski P, et al. Adsorption of the dye Remazol Red 198 (RR198) by O-carboxymethylchitosan-N-lauryl/γ-Fe₂O₃ magnetic nanoparticles. *Arab J Chem* [Internet]. Available from: <http://www.sciencedirect.com/science/article/pii/S1878535215002683>
10. Kumar Gupta V, Agarwal S, Asif M, Fakhri A, Sadeghi N. Application of response surface methodology to optimize the adsorption performance of a magnetic graphene oxide nanocomposite adsorbent for removal of methadone from the environment. *J Colloid Interface Sci.* 2017 Jul 1;497:193–200.
11. Wu W, Jiang CZ, Roy VAL. Designed synthesis and surface engineering strategies of magnetic iron oxide nanoparticles for biomedical applications. *Nanoscale.* 2016;8(47):19421–74.
12. Draget KI, Taylor C. Chemical, physical and biological properties of alginates and their biomedical implications. *Diet Fibre Bioact Polysacch.* 2011 Mar;25(2):251–6.
13. Remminghorst U, Rehm BHA. Bacterial alginates: from biosynthesis to applications. *Biotechnol Lett.* 2006;28(21):1701–12.
14. Rehm BHA, Valla S. Bacterial alginates: biosynthesis and applications. *Appl Microbiol Biotechnol.* 1997;48(3):281–8.
15. Zare M, Ramezani Z, Rahbar N. Development of zirconia nanoparticles-decorated calcium alginate hydrogel fibers for extraction of organophosphorous pesticides from water and juice samples: Facile synthesis and application with elimination of matrix effects. *J Chromatogr A.* 2016 Nov 18;1473:28–37.
16. Bunkoed O, Nurerk P, Wannapob R, Kanatharana P. Polypyrrole-coated alginate/magnetite nanoparticles composite sorbent for the extraction of endocrine-disrupting compounds. *J Sep Sci.* 2016;39(18):3602–9.

17. Chaodao Li, Jianjiang Lu, Shanman L, Yanbin Tong, Bangce Ye. Synthesis of Magnetic Microspheres with Sodium Alginate and Activated Carbon for Removal of Methylene Blue. *Materials*. 2017;84.
18. Pittermannova A, Ruberova Z, Zadrazil A, Bremond N, Bibette J, Stepanek F. Microfluidic fabrication of composite hydrogel microparticles in the size range of blood cells. *RSC Adv*. 2016;6(105):103532–40.
19. Rocher V, Siaugue J-M, Cabuil V, Bee A. Removal of organic dyes by magnetic alginate beads. *Water Res*. 2008 Feb;42(4–5):1290–8.
20. Tao Hu, Qinze Liu, Tingting Gao, Kaijie Dong, Gang Wei, and Jinshui Yao Facile Preparation of Tannic Acid–Poly(vinyl alcohol)/Sodium Alginate Hydrogel Beads for Methylene Blue Removal from Simulated Solution *ACS Omega* **2018** 3(7), 7523-7531 DOI: 10.1021/acsomega.8b00577
21. He J, Cui A, Ni F, Deng S, Shen F, Yang G. A novel 3D yttrium based-graphene oxide-sodium alginate hydrogel for remarkable adsorption of fluoride from water. *J Colloid Interface Sci*. 2018 Dec 1;531:37–46.
22. Nan Wang, Li-Ye Yang, Yang-guang Wang and Xiao-kun Ouyang Fabrication of Composite Beads Based on Calcium Alginate and Tetraethylenepentamine-Functionalized MIL-101 for Adsorption of Pb(II) from Aqueous Solutions *Polymers* 2018, 10(7), 750; <https://doi.org/10.3390/polym10070750>
23. Yi K, Fan Z, Tang J, Chen A, Shao J, Peng L, et al. The elucidation of surrounding alginate gels on the pollutants degradation by entrapped nanoscale zero-valent iron. *Colloids Surf B Biointerfaces*. 2018 Nov 1;171:233–40.
24. Gjipalaj J, Alessandri I. Easy recovery, mechanical stability, enhanced adsorption capacity and recyclability of alginate-based TiO₂ macrobead photocatalysts for water treatment. *J Environ Chem Eng*. 2017 Apr 1;5(2):1763–70.
25. Liao S-H, Liu C-H, Bastakoti BP, Suzuki N, Chang Y, Yamauchi Y, et al. Functionalized magnetic iron oxide/alginate core-shell nanoparticles for targeting hyperthermia. *Int J Nanomedicine*. 2015;10:3315–28.
26. Ma H, Qi X, Maitani Y, Nagai T. Preparation and characterization of superparamagnetic iron oxide nanoparticles stabilized by alginate. *Int J Pharm*. 2007 Mar 21;333(1–2):177–86.
27. Mohammadi A, Daemi H, Barikani M. Fast removal of malachite green dye using novel superparamagnetic sodium alginate-coated Fe₃O₄ nanoparticles. *Int J Biol Macromol*. 2014 Aug;69:447–55.

28. Peng N, Wu B, Wang L, He W, Ai Z, Zhang X, et al. High drug loading and pH-responsive targeted nanocarriers from alginate-modified SPIONs for anti-tumor chemotherapy. *Biomater Sci.* 2016;4(12):1802–13.
29. Castelló J, Gallardo M, Busquets MA, Estelrich J. Chitosan (or alginate)-coated iron oxide nanoparticles: A comparative study. *Colloids Surf Physicochem Eng Asp.* 2015 Mar 5;468:151–8.
30. Sidhu, P. S. Dissolution of iron oxides and oxyhydroxides in hydrochloric and perchloric acids. *Clays and Clay Minerals.* 1981 29(4) : 269-276,
31. Ravindra Kumar Gautam, Mahesh Chandra Chattopadhyaya. *Advanced Nanomaterials for Wastewater Remediation.* CRC Press. 2016. 454 p.
32. Lagoa R, Rodrigues JR. Evaluation of Dry Protonated Calcium Alginate Beads for Biosorption Applications and Studies of Lead Uptake. *Appl Biochem Biotechnol.* 2007 Nov 1;143(2):115–28.
33. Lamelas C, Avaltroni F, Benedetti M, Wilkinson KJ, Slaveykova VI. Quantifying Pb and Cd Complexation by Alginates and the Role of Metal Binding on Macromolecular Aggregation. *Biomacromolecules.* 2005 Jul 23;6(5):2756–64.
34. Massart R. Preparation of aqueous magnetic liquids in alkaline and acidic media. *IEEE Trans Magn.* 1981;17(2):1247–8.
35. Bee A, Massart R, Neveu S. Synthesis of very fine maghemite particles. *J Magn Magn Mater.* 1995;149:6–9.
36. Cabuil V, Perzynski R. Particle size determination in magnetic fluids. In: Berkovski VB and B, editor. *Magnetic Fluids and Handbook applications.* New York and Wallingford (UK): begell house; 1996.
37. Foner S, Jr. EJM. Very Low Frequency Integrating Vibrating Sample Magnetometer (VLFVSM) with High Differential Sensitivity in High dc Fields. *Rev Sci Instrum.* 1968;39:171.
38. Bée A, Obeid L, Mbolantenaina R, Welschbillig M, Talbot D. Magnetic chitosan/clay beads: A magsorbent for the removal of cationic dye from water. *J Magn Magn Mater.* 2017 Jan 1;421:59–64.
39. Bacri J-C, Perzynski R, Salin D, Cabuil V, Massart R. Magnetic colloidal properties of ionic ferrofluids. *J Magn Magn Mater.* 1986 Nov 1;62(1):36–46.
40. Xu XQ, Shen H, Xu JR, Xie MQ, Li XJ. The colloidal stability and core-shell structure of magnetite nanoparticles coated with alginate. *Appl Surf Sci.* 2006 Dec 15;253(4):2158–64.

41. Ahmadi M, Rahmani H, Takdastan A, Jaafarzadeh N, Mostoufi A. A novel catalytic process for degradation of bisphenol A from aqueous solutions: A synergistic effect of nano-Fe₃O₄@Alg-Fe on O₃/H₂O₂. *Process Saf Environ Prot.* 2016;104:413–21.
42. Mohammadi A, Daemi H, Barikani M. Fast removal of malachite green dye using novel superparamagnetic sodium alginate-coated Fe₃O₄ nanoparticles. *Int J Biol Macromol.* 2014 Aug;69:447–55.
43. Zhang J, Ji Q, Shen X, Xia Y, Tan L, Kong Q. Pyrolysis products and thermal degradation mechanism of intrinsically flame-retardant calcium alginate fibre. *Polym Degrad Stab.* 2011 May;96(5):936–42.
44. Mak S-Y, Chen D-H. Fast adsorption of methylene blue on polyacrylic acid-bound iron oxide magnetic nanoparticles. *Dyes Pigments.* 2004 61(1):93–8.
45. Bée A, Talbot D, Abramson S, Dupuis V. Magnetic alginate beads for Pb(II) ions removal from wastewater. *J Colloid Interface Sci.* 2011 Oct 15;362(2):486–92.
46. Ponton A, Bee A, Talbot D, Perzynski R. Regeneration of thixotropic magnetic gels studied by mechanical spectroscopy: the effect of the pH. *J Phys Condens Matter.* 2005;17:1–16.
47. N. Kannan et M. M. Sundaram Kinetics and mechanism of removal of methylene blue by adsorption on various carbons—a comparative study. *Dyes Pigments.* 2001; 51(1): 25- 40.
48. M. Auta et B. H. Hameed, Chitosan–clay composite as highly effective and low-cost adsorbent for batch and fixed-bed adsorption of methylene blue. *Chem. Eng. J.* 2014; 237: 352-361.